Results in Optics 13 (2023) 100522

Contents lists available at ScienceDirect

Results in Optics

journal homepage: www.sciencedirect.com/journal/results-in-optics

Compact two-port antenna with high isolation based on the defected ground for THz communication

Anubhav Kumar [a,*], Divya Saxena [b], Pankaj Jha [c], Navneet Sharma [d]

[a] Department of Electronics and Communication Engineering, Raj Kumar Goel Institute of Technology & Management, Ghaziabad, Uttar Pradesh, India
[b] Applied Science & Humanities, ABES Engineering College, Ghaziabad, Uttar Pradesh, India
[c] Department of Electronics and Communication Engineering, IIMT College of Engineering, Greater Noida, Uttar Pradesh, India
[d] Department of Electronics and Communication Engineering, ABES Engineering College, Ghaziabad, Uttar Pradesh, India

A R T I C L E I N F O

Keywords:
MIMO antenna
Defected ground
THz application
Isolation enhancements
Open-ended slots

A B S T R A C T

The two-port antenna is designed for THz communication where isolation is achieved with the defective ground. The radiator of the two-port antenna is inspired by the half-cutting technology which reduces the size and makes it a compact antenna. The T-shaped stub and open-ended slot are used to modify the capacitive and inductive reactance which diminish and discontinued the surface current to improve the port isolation. The T-shaped stub improves the electric length of the ground and enhances the port isolation by up to 3.4 dB and open-ended slot in the ground is used to weaken the mutual current and create the non-uniform current which intensifications the port isolation up to 7.7 dB at 2.2 THz. The dimensions of the design is 100 μm × 105 μm and the edge distance of the antennas is only 0.20λ with maximum isolation is 30 dB at 2.2 THz. The bandwidth of the two-port antenna is 1.74 THz to 2.52 THz that can be applicable in wireless communication applications.

1. Introduction

The increasing bandwidth, high-speed communication, low latency, and large channel capacity demands of users in wireless communication have led to the new requirement, which has led to a focus on THz frequencies. The bandwidth from 0.1 to 10 THz can fulfil the future demands of 6G communication with low interference (Han et al., 2019; Kumar and Saxena, 2020). However, due to the high molecular absorption in the outdoor atmosphere and spreading loss, the signal will have a higher efficiency for use in short-distance communication (Akyildiz et al., 2018). The use of THz frequency in places like the military, biomedical, and security shows its potential in communication, sensing, and imaging (Hwu et al., 2013; Woolard et al., 2005) which can establish new dimensions in communication. However, the new yield requirements cannot be met with single-element antennas and MIMO antennas are the only solution that can fulfil these requirements. According to the analysis, the MIMO antenna used in THz communication is required to have compact, high isolation, and less complicated structure. In (Singhal, 2020), the dimension of the design is 800 μm × 1170 μm for the THz band where the antenna is designed on spatial diversity arrangement with higher than 30 dB port isolation. The substrate to design the antenna is polyamide where copper is used for conducting elements. In (Rubani et al., 2020), the radiator is separated by the λ/4 distance and used RTDuroid/6010 material to obtain the narrow band THz frequencies when no decoupling is used for isolation and efficiency is not reported. In (Saxena et al., 2020), the dimension of the design is 1000 μm × 1400 μm is used where the elliptical-shaped radiator with partial ground loaded on the RT5880 substrate. The two-port antenna obtained 70 % efficiency and more than 25 dB isolation with help of the defective ground. In (Okan, 2021), Rogers RO4835-T is utilized for two-port antenna for 0.095–0.205 THz frequency with an elliptical-shaped radiator without common ground. The port distance used to obtain the isolation is more than 17 dB. In (Keshwala, 2021), a sinusoidal slot in the square-shaped radiator is introduced for the THz two-port antenna where unconnected ground and port distance influence the isolation. In (Varshney et al., 2019), graphene patch loaded microstrip fed two-port antenna is designed for THZ application to insure pattern diversity. The port distance of the antenna reduces the surface current and helps to provide port isolation of up to 25 dB. In (Maurya et al., 2023), silicon dioxide is used to design the two-port antenna with microstrip-fed and ring slot in the ground to increase the impedance bandwidth. The graphene-based decoupling strip is used to weaken the coupling which improves the isolation. In (Vasu Babu et al., 2022), the tree-shaped radiator with the partial ground is used for two-

* Corresponding author.
E-mail address: rajput.anubhav@gmail.com (A. Kumar).

https://doi.org/10.1016/j.rio.2023.100522
Received 1 July 2023; Received in revised form 15 August 2023; Accepted 1 September 2023
Available online 4 September 2023

port antenna where the unconnected ground is used for isolation improvement. The efficiency of the antenna is low with Polyimide material. In (Vijayalakshmi et al., 2021), graphene is loaded on the Polyimide to design the triple band antenna where the parasitic meander line is used to diminish the coupling and help to achieve isolation up to 15 dB. In (Babu et al., 2022), the dimension of the design is 600 μm × 300 μm with unconnected ground antenna. The port-isolation achieved up to 25 dB with Polyimide material. The analysis of the literature, a compact two-port antenna with Polyimide substrate and copper conducting material is used for THz applications in this paper. This design is robust in fabrication due to compact size, high values of total as well as radiation efficiency and used polyimide material as a substrate. The fractional bandwidth of the two-port antenna is 35 % with high efficiency as well as port isolation whereas miniaturization of the two-port antenna is achieved with half-cutting technology. The decoupling technology is designed with simple structure without complexity where the distance

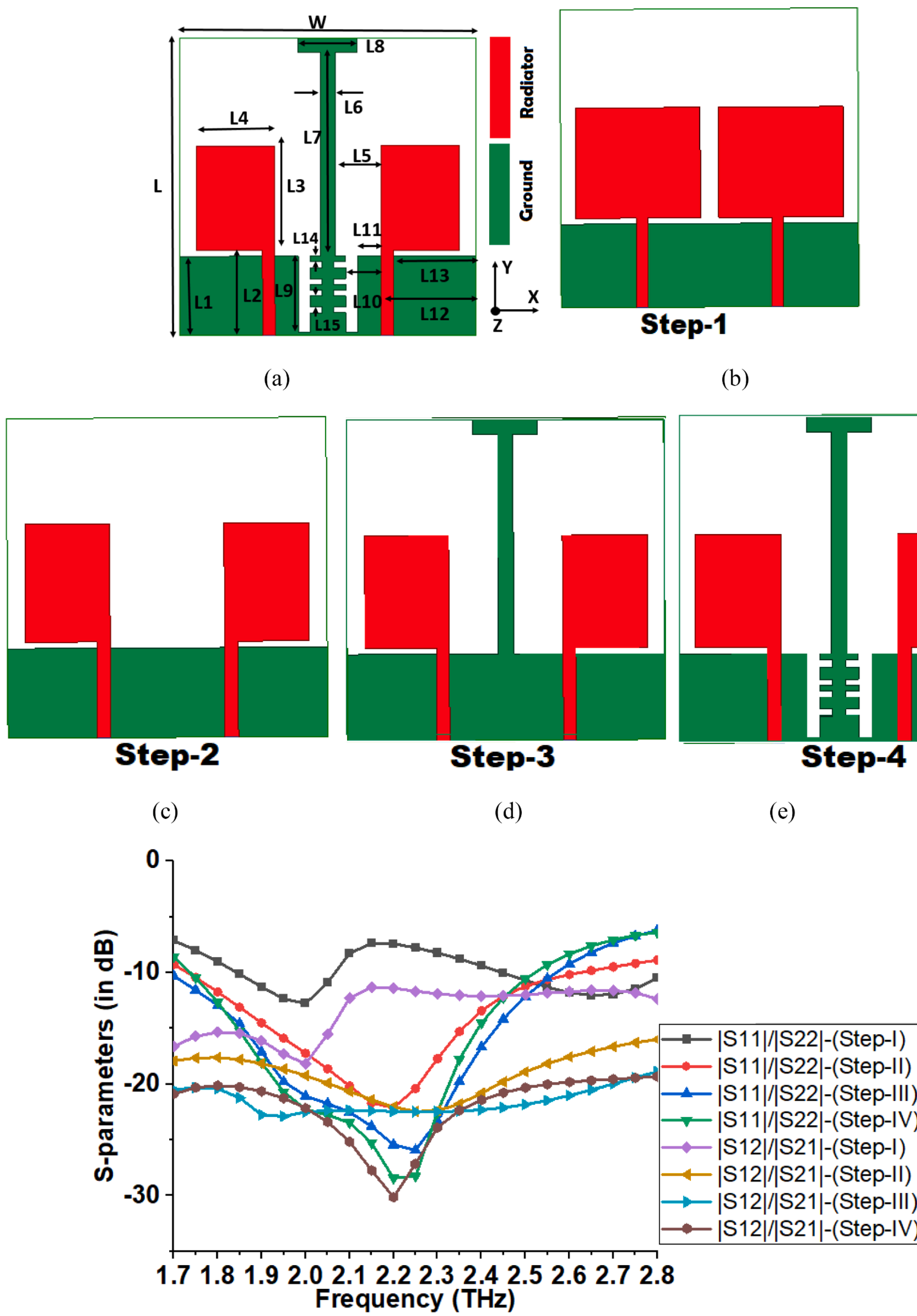

Fig. 1. THz two-port antenna (a) Prototype (b-e) evolution steps (f) S-parameters (g) Surface current at 2.2 THz.

(f)

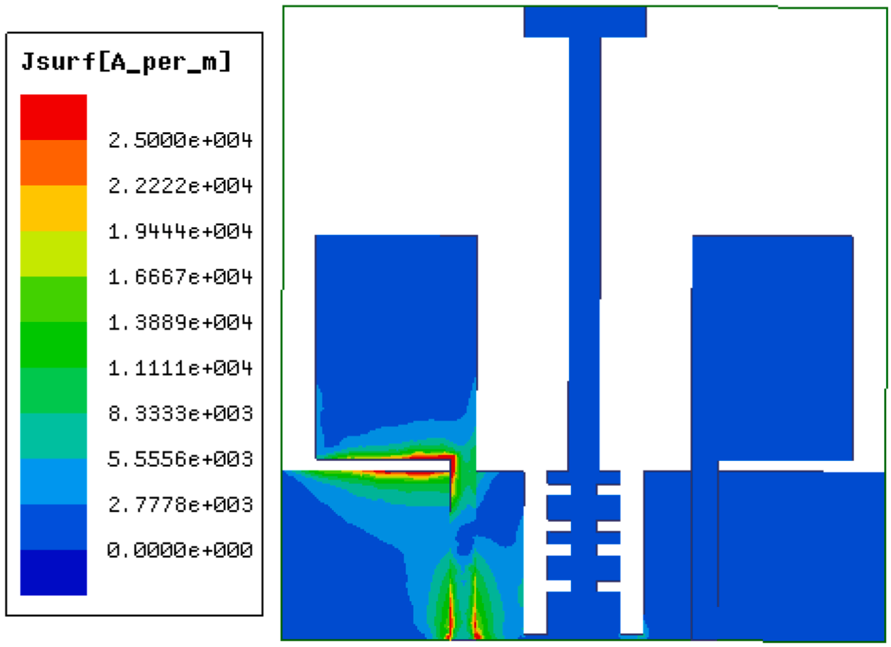

(g)

Fig. 1. (*continued*).

of the antenna elements is only 0.20λ when the unconnected ground and distance between antenna elements is more than 0.25λ is common in literature. Therefore the design of the two-port antenna creates the impact on specific industries in THz applications. The technical advancement and novelty of the work is elaborated below.

- The polyimide substrate with copper conducting material is used where the maximum efficiency is achieved with 96 % at 2 THz.
- The radiator is inspired by the half-cutting technology which reduces the size of the antenna.
- The distance from edges of the antennas is only 0.20λ where the isolation is greater than 20 dB.
- The T-shaped stub improves the electric length of the ground and enhances the port isolation by up to 3.4 dB.
- The open-ended slots in the ground is used to weaken the mutual current and create the non-uniform current which intensifies the port isolation up to 7.7 dB at 2.2 THz.

2. THz antenna design

The two-port antenna based on the defective ground is designed on the HFSS V13 software. The Polyimide substrate is utilized with relative permittivity of 3.5. The tangent loss and thickness of the material are 0.008 and 3.2 μm. Copper is used as a conductive element with a thickness of 35 nm. The dimension of the design of two-port antenna is 100 μm × 105 μm as represented in Fig. 1(a). This work is designed in four evolution step are depicted in Fig. 1(b-e), the s-parameters is represented in Fig. 1 (f) and the parameters of the size are as follows (in the μm): L = 105, W = 100, L1 = 28, L13 = 27.9, L2 =,30 L12 = 32.1, L3 = 37, L11 = 7.9, L4 = 26.5, L10 = 11.4, L5 = 15.4, L9 = 27,L14 = 2,L15 = 4, L6 = 5, L8 = 20, L7 = 72. In the first step-1, a rectangular-shaped radiator is used with a size of 110 μm × 105 μm and the length (L) and width (W) of the radiator are 37 μm and 46 μm. The distance from the edges of the antenna is 8.4 μm. The impedance bandwidth (IBW) is obtain from 1.85 THz to 2.06 THz and 2.45 THz to 2.82 THz with 11 dB isolation. In step-2, the radiator of the two-port antenna is inspired by the half-cutting technology, and the dimension is modified to 100 μm × 105 μm. The distance between the antenna edges is 36 μm (0.20λ) and less than a quarter wavelength of the lower frequency of the antenna. The IBW is 1.74 to 2.62 THz where the isolation is amended due to weaker electric field up to 17 dB. In the third step, the defective ground is introduced in the change in the inductive and capacitive reactance of the antenna due to non-uniform ground. The T-shaped stub is hosted in the ground which increases the isolation by perturbs the ground current and enhancing the electrical size of the ground. The IBW varies from 1.7 THz to 2.55 THz and isolation is enhances up to 20 dB where the maximum value of the isolation is 22.5 dB at the 2 THz. In the final step, the two symmetrical open-ended slots are inserted which diminish the coupling current in the antenna and improve the port isolation. The IBW varies from 1.74 THz to 2.52 THz and isolation is >20 dB where the maximum value of the isolation is 30 dB at the 2.2 THz. The defected ground creates a non-uniform current and creates discontinuity which is used to diminish the surface current as shown in the Fig. 1 (g) where the T-shaped stub and open-ended slot create the non-uniform current, perturbs, and diminish the current from one to two ports. The huge losses, low thermal stability, low electrical insulation, less chemical resistance fabrication complexity due to substrate and complex decoupling structure, low efficiency, unconnected ground are associated in THz antenna design. In this paper, the design and investigation on polyimide substrate with half-cutting technology which reduces the size of the antenna. The high value of efficiency is obtained with the proposed design to overcome the losses. The connected ground can be good choice for MIMO antenna design where the discussed decoupling with the defected ground can overcome the surface wave in between antenna without further complexity. THz bands has high bandwidth which can complete the present bandwidth requirement and useful for short distance communication with high gain and efficiency. THz frequencies have shorter wavelengths which can be effectively used to determine small obstacles in imaging and tracking and may be seen in future applications such as wearable and biomedical applications.

3. Equivalent circuit (EC) model of two-port antenna

EC model is designed to validate the simulated results from HFSS software. The EC model is calculated to determine the lumped component of radiator and the decoupling structure of the two-port antenna. The QUCS software is used to determined and extract the lumped parameters with tuning phenomena for adjusting the RLC value and determine the s-parameters achieved to validate the model. The Rf1/Rf2,Cf1/Cf2 and Lf1/Lf2 are the RLC elements of the microstrip fed where the Cp1/Cp2,Lp1/Lp2,Rp1/Rp2 are the RLC components of the radiator. The RLC components represent the defected ground and coupling is C17, L13 and R1. The EC model with lumped elements is discussed in the Fig. 2 (a) and the extracted s-parameters from EC model and HFSS are illustrated in the Fig. 2(b) which validate the results.

4. Results and analysis

The two-port antenna is based on the half-cutting technology and isolation enhancement by the defected ground which is introduced by the T-shaped stub and open-ended slot. The |S11| of the two-port antenna is 1.74 THz to 2.52 THz as represented in Fig. 3 (a) where the maximum value of isolation is 30 dB which shows the minimum coupling current between antennas. The isolation (|S21|) is amended up to 20 dB in the operating range. The fabrication methods, testing and measurement of the THz antenna in micro/nanoscale have high challenges. Recently only fabrication process is discussed in graphene absorber (Varshney and Giri, 2021), THz antenna (Ashvanth and Partibane, 2021; Ali et al., 2022) which are presently yet to be investigate and restricted (Ashvanth and Partibane, 2021) in the design of antenna. The implementation of THz antenna with compact size where the fabrication accuracy at such a small structure is a complex process whereas the power consumption is high which limits the application of THz antenna (Rasilainen, 2023; Han et al., 2021). The copper as a conducting element suffers high propagation loss and low efficiency which is again a limitation of copper in THz antenna (Dash and Patnaik, 2018) where the metallic contact and antenna matching to channel become very challenging at the THz frequency. The efficiency is discussed using radiated power and the accepted power. The efficiency is an important concern in the THz frequencies where the loss is higher. The efficiency of the proposed antenna achieved more than 92 % where the maximum value is 96 % at 2 THz as illustrated in Fig. 3 (b). The two-port antenna is an omnidirectional antenna and compact, due to which the gain from 2.6 dB to 4.4 dB in the entire operating range illustrated in

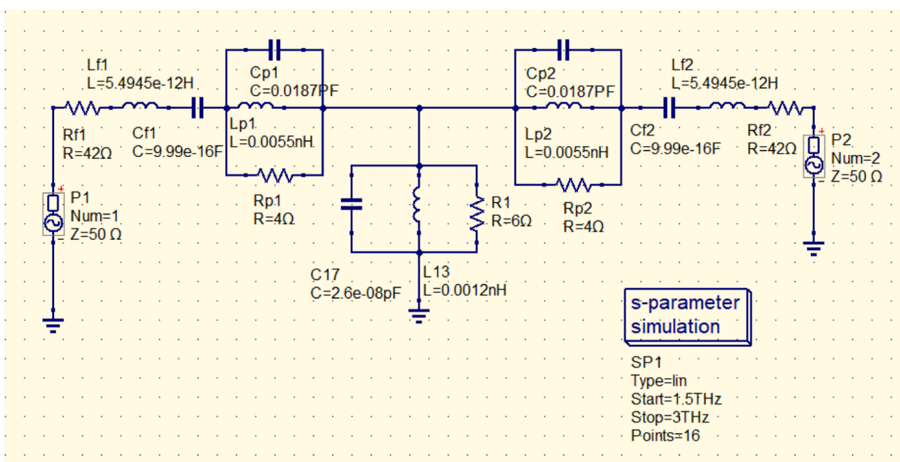

(a)

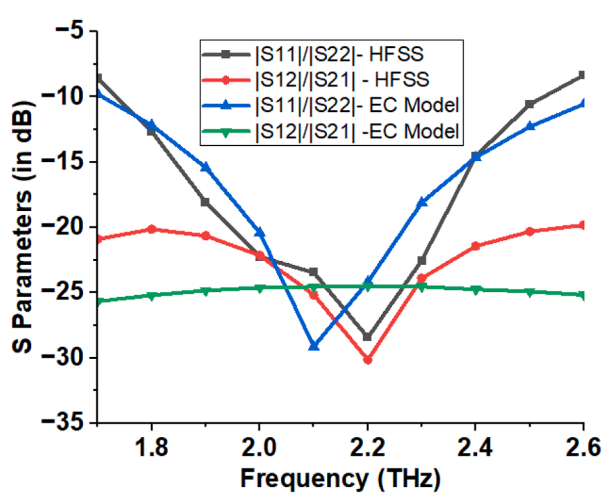

(b)

Fig. 2. EC model design and results (a) EC model with lumped elements (b) S-parameters from HFSS and EC model.

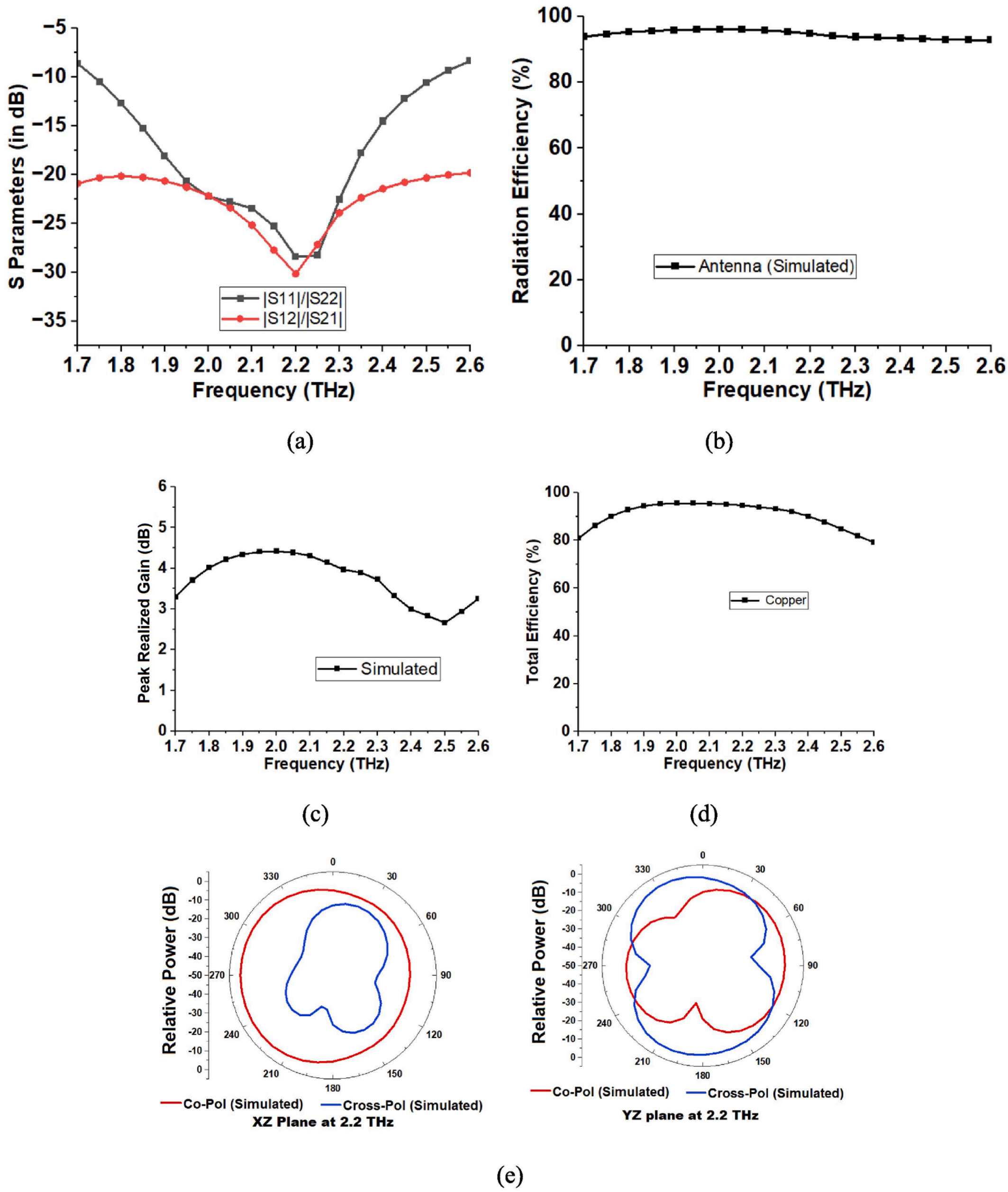

Fig. 3. Two-port antenna results (a) S-parameters (b) Radiation efficiency (c) Gain (d) Total efficiency (e) radiation patterns.

Fig. 3 (c). The gain of the antenna could be a limitation of THz application but with higher efficiency, compact size, easy decoupling which reduces the complexity in fabrication, the proposed two-port antenna perform better with high channel capacity and reduced multipath fading. To keep in the mind of the fabrication tolerance in THz antenna, the polyimide material used as a substrate due to micro-scaling applications, which is having good electrical insulation properties, thermal stability, chemical resistance and mechanical toughness (Babu et al., 2022). The total efficiency of a two-port antenna is also determined for accommodate the fabrication tolerance (Ashvanth and Partibane, 2021) which is important to determine the effectiveness of the antenna in THz bands applications from the antenna's radiation efficiency and mismatch efficiency as illustrated in the eq. 1–3 (Huang, 2021). The total efficiency of the antenna is greater than 80% and maximum value is 95.5% as depicted in the Fig. 3(d) which may exhibits better fabrication tolerances in THz applications.

$$\text{Total Efficiency }(\eta_T) = \text{Radiation Efficiency}(\eta_R) \times \text{Mismatch Efficiency}(\eta_m) \quad (1)$$

and

$$\eta_m = 1 - |\Gamma|^2 \quad (2)$$

$$\Gamma = \frac{Z_{in} - Z_0}{Z_{in} + Z_0} \quad (3)$$

where Zin and Zo are the input and characteristics impedance of the transmission line. The two-port antenna radiation pattern in normalized values is determined in XZ and YZ planes where the omnidirectional radiation pattern at 2.2 THz is observed as depicted in Fig. 3(e). The Table 1 represented the comparative investigation with literature work of the proposed work in different frequency bands and materials. The Polyimide/ polyamide (Singhal, 2020; Keshwala, 2021; Vasu Babu et al., 2022; Vijayalakshmi et al., 2021; Babu et al., 2022) material is used

Table 1
Comparative analysis of two-port THz antenna.

S.No (Year)	Material	Size (μmx μm)	Bandwidth (GHz	Efficiency (%)	Isolation (dB)	Technology
Proposed	Polyimide	100 × 105	1.74 to 2.52	92	20	Defected ground
(Singhal, 2020)	polyamide	800 × 1170	0.25–15.4	–	30	Distance between antenna
(Rubani et al., 2020)	RT/Duriod6010	36 × 35	8.84	–	22	Distance of λ/4.
(Saxena et al., 2020)	RT5880	1000 × 1400	0.33–10	70	25	Inverted-L-shaped stub
(Okan, 2021)	Rogers RO4835-T	2000 and 1000	0.095–0.205	94	17	Unconnected ground
(Keshwala, 2021)	Polyimide	100 × 180	1.01 to 2.21, 5.64 to 37.5	–	20	Unconnected ground
(Varshney et al., 2019)	silicon dioxide	60x40	1.76–1.8	–	25	Port distance
(Maurya et al., 2023)	silicon dioxide	40x20	5.68–6.51	90.17	17.15	Graphene based
(Vasu Babu et al., 2022)	Polyimide	600 × 300	0.276–0.711	20	20	Unconnected ground
(Vijayalakshmi et al., 2021)	polyimide	50x40	2.3, 3.2 and 4.5	60	15	Parasitic resonator
(Babu et al., 2022)	Polyimide	600x300	0.35–0.75	82	25	Unconnected ground

where (Singhal, 2020; Keshwala, 2021) is not reported the antenna efficiency, (Vasu Babu et al., 2022; Vijayalakshmi et al., 2021) having lower efficiency, and (Babu et al., 2022) has used the higher antenna size with the unconnected ground to design the MIMO antenna. In, [7, 8 and 9] used RT6010/ RT5880/ Rogers RO4835-T but efficiency of is not discussed and having larger size of the MIMO antenna. In (Varshney et al., 2019; Maurya et al., 2023) have used silicon dioxide and achieved good efficiency with 90% but have less than 20 dB isolation. As per analysis of the literature where the many work have not discussed the efficiency of the MIMO antenna also having lower isolation with larger dimensions as well as designed with unconnected ground where the presented work discussed about the significance of the Polyimide substrate as well as designed with high efficiency as well as high isolation without complicated decoupling. Therefore, the proposed work may be effective in wireless, imaging and tracking application with minimum multipath fading and high channel capacity.

5. MIMO parameters

The Envelope Correlation Coefficient (ECC) depends upon the mutual coupling of the multiple-element antenna and is effective when the mutual coupling is minimum. The practical ECC should be low as possible and ideally zero when low correlation in the MIMO antenna or antenna element is independent. In other words, ECC has defined the antenna correlation between the adjacent antenna. The ECC can be extracted from the S-parameters as discussed in eq.4 where a 0.5 value of ECC is an acceptable limit for practical applications. The ECC of the proposed Two-port antenna is under 0.006 as illustrated in Fig. 4 (a) and in under the acceptable limit.

$$ECC = \frac{\left|S_{11}^{*}S_{12} + S_{21}^{*}S_{22}\right|^{2}}{\left(1 - |S_{11}|^{2} - |S_{21}|^{2}\right)\left(1 - |S_{22}|^{2} - |S_{12}|^{2}\right)} \tag{4}$$

If the signal is arriving separately from multiple propagation paths

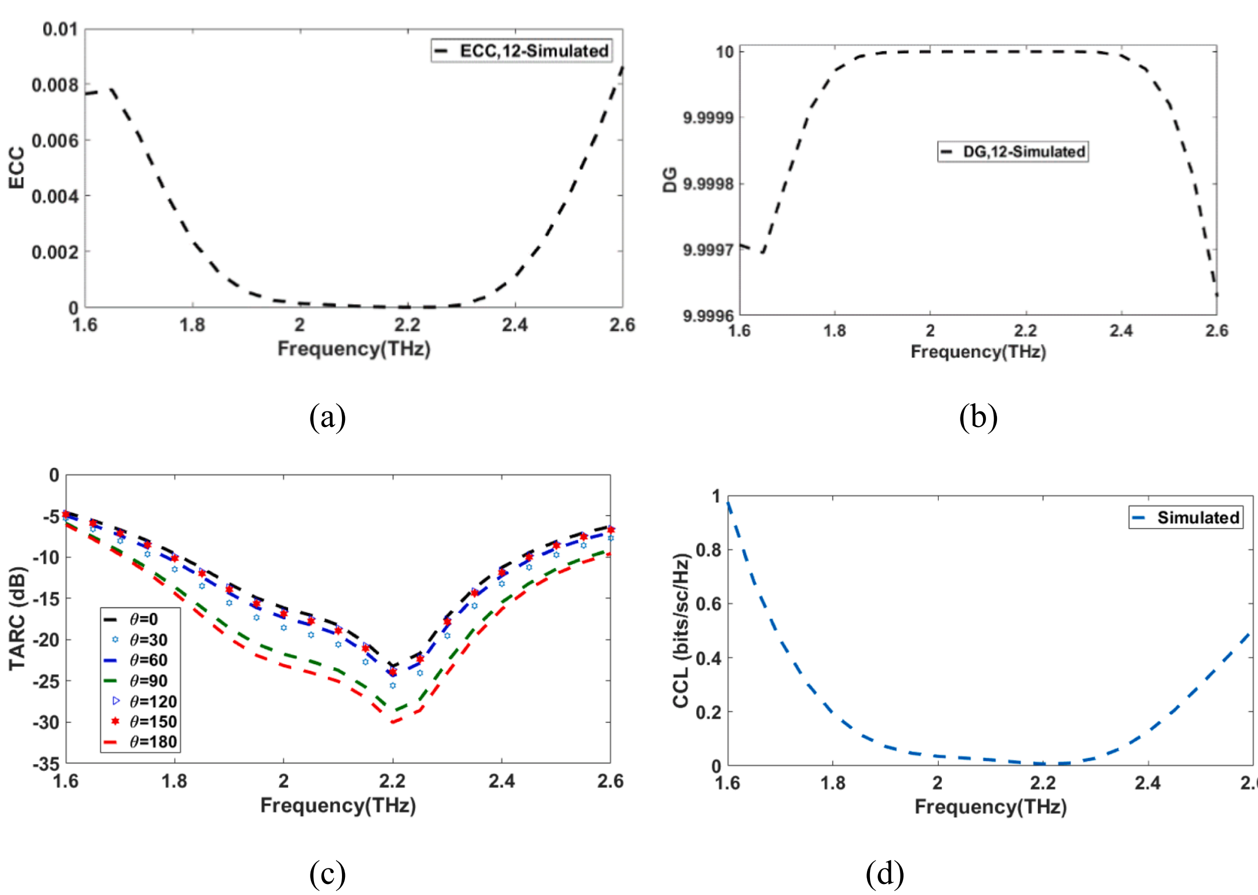

Fig. 4. MIMO parameters (a) ECC (b) DG (c) TARC (d) CCL.

and is not correlated with each other, it shows better SNR at the receiver which can be derived from the Diversity Gain (DG). The DG is determined by the ECC as illustrated in the eq.5, represented the SNR of the multiple-element antenna to the single antenna where the value of the DG should be close to 10 dB for practical applications. The DG of the two-port antenna is close to 10 dB.

$$\boldsymbol{DG} = 10\sqrt{1 - |\boldsymbol{ECC}|^2} \tag{5}$$

The total active reflection coefficient (TARC) is the effective medium to determine the efficiency and bandwidth of the multiple-element antenna where the s-parameters is not sufficient. The TARC is represented by the individual square root of reflected and the incident power. The size s-parameters matrix increases with the increases in the antenna element therefore TARC is representing the all information of N number of the port of s-parameters and the influence of the feeding phase represented in Eq.(6). The results showing in Fig. 4 (c), the minimum effect in the s-parameters and showing acceptable results.

$$TARC = \frac{\sqrt{\sum_{i=1}^{N}|b_i|^2}}{\sqrt{\sum_{i=1}^{N}|a_i|^2}}$$

$$\boldsymbol{TARC} = \sqrt{\left(|\boldsymbol{S}_{11} + \boldsymbol{S}_{12}\boldsymbol{e}^{j\theta}|^2 + |\boldsymbol{S}_{22}\boldsymbol{e}^{j\theta} + \boldsymbol{S}_{21}|^2\right)/\sqrt{2}} \tag{6}$$

The high channel capacity can be achieved by the MIMO antenna in multipath propagation compared to the single antenna. The Channel Capacity Loss (CCL) is ideally equal to zero but should be less than 0.4 bits/sec/Hz as illustrated in the Fig. 4 (d). The CLL depends on the correlation coefficient ($\boldsymbol{\psi}^{\boldsymbol{R}}$) (Mukherjee and Chauhan, 2021; Sharawi, 2014) is the receiving antenna and helps to determine the diversity enactment of the antenna which is calculated from the eq.7. The MIMO antenna has higher channel capacity compare to single antenna element as well reduced the multipath fading when the path of the received signals are different. The channel capacity is calculated from the channel matrix of the antenna elements. The channel matrix and the antenna element characteristics is reduced when the isolation is lower that why the CCL is reduced where the CCL is representing the highest information accessible rate at which signal or information can be send or transmitted with minimum or without loss.

$$\boldsymbol{CCL} = -\boldsymbol{log}_2\boldsymbol{det}(\boldsymbol{\psi}^{\boldsymbol{R}}) \tag{7}$$

Where

$$\boldsymbol{\psi}^R = \begin{pmatrix} \boldsymbol{\psi}_{11} & \boldsymbol{\psi}_{12} \\ \boldsymbol{\psi}_{21} & \boldsymbol{\psi}_{22} \end{pmatrix} \tag{8}$$

and

$$\boldsymbol{\psi}_{11} = 1 - (|\boldsymbol{S}_{11}|^2 - |\boldsymbol{S}_{12}|^2$$

$$\boldsymbol{\psi}_{22} = 1 - (|\boldsymbol{S}_{22}|^2 - |\boldsymbol{S}_{21}|^2$$

$$\boldsymbol{\psi}_{21} = -(\boldsymbol{S}^*_{22}\boldsymbol{S}_{21} + \boldsymbol{S}^*_{12}\boldsymbol{S}_{11})$$

$$\boldsymbol{\psi}_{12} = -(\boldsymbol{S}^*_{11}\boldsymbol{S}_{12} + \boldsymbol{S}^*_{21}\boldsymbol{S}_{22})$$

6. Conclusion

The compact and the two-port antenna for THz communication with high isolation is proposed. The dimension of the antenna is 100 μm × 105 μm and the distance of the edge of the antenna is only 0.20λ. The half cutting technology is used to reduce the size of the antenna. The open-ended slot and the T-shaped stub is utilising to reduce the surface current of the antenna where the maximum isolation is achieve 30 dB. The bandwidth of the two-port antenna is 1.74 THz to 2.52 THz with port isolation of higher than 20 dB. The MIMO characteristics of the two-port antenna is in suitable limits therefore the two-port antenna can effectively work in wireless applications.

Funding

This work did not receive any funding.

8. Ethics approval

This research study complied with the ethical standards.

Declaration of Competing Interest

The authors declare that they have no known competing financial interests or personal relationships that could have appeared to influence the work reported in this paper.

Data availability

No data was used for the research described in the article.

References

Akyildiz, I.F., Han, C., Nie, S., 2018. Combating the distance problem in the millimeter wave and terahertz frequency bands. IEEE Commun. Mag. 56 (6), 102–108.
Ali, M.F., Bhattacharya, R., Varshney, G., 2022. Tunable four-port MIMO/self-multiplexing THz graphene patch antenna with high isolation. Opt. Quant. Electron. 54 (12), 822.
Ashvanth, B., Partibane, B., 2021. Multiband characterized high gain MIMO antenna for terahertz applications. Opt. Quant. Electron. 53 (8), 460.
Babu, K.V., Das, S., Sree, G.N.J., Madhav, B.T.P., Patel, S.K.K., Parmar, J., 2022. Design and optimization of micro-sized wideband fractal MIMO antenna based on characteristic analysis of graphene for terahertz applications. Opt. Quant. Electron. 54 (5).
Dash, S., Patnaik, A., 2018. Material selection for TH z antennas. Microw. Opt. Technol. Lett. 60 (5), 1183–1187.
Han, C., Wu, Y., Chen, Z. and Wang, X., 2019. Terahertz communications (TeraCom): Challenges and impact on 6G wireless systems. *arXiv preprint arXiv:1912.06040*, (2019).
Han, C., Yan, L., Yuan, J., 2021. Hybrid beamforming for terahertz wireless communications: challenges, architectures, and open problems. IEEE Wirel. Commun. 28 (4), 198–204.
Huang, Y.i., 2021. Antennas: From Theory to Practice. John Wiley & Sons.
Hwu, S.U., deSilva, K.B., Jih, C.T., 2013. Terahertz (THz) wireless systems for space applications. In: *2013 IEEE Sensors Applications Symposium ProceedIngs*. IEEE, pp. 171–175.
Keshwala, U., 2021. Microstrip line fed sinusoidal tapered square shaped MIMO antenna for THz applications. Optik 247, 167905.
Kumar, A., Saxena, D., 2020. Compact UWB microstrip antenna for THz communication application. In: *2020 9th International Conference System Modeling and Advancement in Research Trends (SMART)*. IEEE, pp. 388–391.
Maurya, N.K., Kumari, S., Pareek, P., Singh, L., 2023. Graphene-based frequency agile isolation enhancement mechanism for MIMO antenna in terahertz regime. Nano Commun. Networks 35, 100436.
Mukherjee, B., Chauhan, M., 2021. Dielectric Resonator Antennas. Artech House.
Okan, T., 2021. High efficiency unslotted ultra-wideband microstrip antenna for sub-terahertz short range wireless communication systems. Optik 242, 166859.
Rasilainen, K., et al., 2023. Hardware aspects of Sub-THz antennas and reconfigurable intelligent surfaces for 6G applications. IEEE J. Sel. Areas Commun.
Rubani, Q., Gupta, S.H., Rajawat, A., 2020. A compact MIMO antenna for WBAN operating at Terahertz frequency. Optik 207, 164447.
Saxena, G., Awasthi, Y.K., Jain, P., 2020. High isolation and high gain super-wideband (0.33-10 THz) MIMO Antenna for THz applications. Optik 223, 165335.
Sharawi, M.S., 2014. Printed MIMO Antenna Engineering. Artech House.
Singhal, S., 2020. Tetradecagonal ring shaped terahertz superwideband MIMO antenna. Optik 208, 164066.
Varshney, G., Giri, P., 2021. Bipolar charge trapping for absorption enhancement in a graphene-based ultrathin dual-band terahertz biosensor. Nanoscale Advances 3 (20), 5813–5822.
Varshney, G., Gotra, S., Pandey, V.S., Yaduvanshi, R.S., 2019. Proximity-coupled two-port multi-input-multi-output graphene antenna with pattern diversity for THz applications. Nano Commun. Networks 21, 100246.

Vasu Babu, K., Das, S., Varshney, G., Sree, G.N.J., Madhav, B.T.P., 2022. A micro-scaled graphene-based tree-shaped wideband printed MIMO antenna for terahertz applications. J. Comput. Electron. 21 (1), 289–303.

Vijayalakshmi, K., Selvi, C.K., Sapna, B., 2021. Novel tri-band series fed microstrip antenna array for THz MIMO communications. Opt. Quant. Electron. 53, 1–13.

Woolard, D.L., Brown, R., Pepper, M., Kemp, M., 2005. Terahertz frequency sensing and imaging: A time of reckoning future applications? Proc. IEEE 93 (10), 1722–1743.